Entanglement structure of non-equilibrium steady states

Brian Swingle, Sam Mumford, Raghu Mahajan
Department of Physics, Stanford University, Palo Alto California, USA

Daniel Freeman
Department of Physics, University of California, Berkeley, Berkeley California, USA

Norm M. Tubman
Department of Physics, University of Illinois, Urbana, Illinois, USA
(Dated: February 1, 2016)

This is the first in a series of papers whose purpose is to obtain transport properties of interacting quantum liquids, specifically electrical and thermal conductivities, by computing the non-equilibrium steady state of the system biased by contacts. Our approach is based on the structure of quantum entanglement in the current carrying state. With reasonable physical assumptions we show that current carrying non-equilibrium steady states close to equilibrium are lightly entangled. We further argue that the steady state can be represented in a computationally efficient form known as tensor network state. Once we know that the steady state has an efficient tensor network representation, the question becomes how to find the steady state. We argue that the non-equilibrium steady state may be found by dynamically evolving the system within a manifold of appropriate low entanglement states. A physically realistic law of dynamical evolution is markovian open system dynamics. Besides establishing these general results, we make a systematic exploration of this approach to transport in a well-studied free fermion model where comparisons with the literature are possible. We conclude with a discussion of the prospects of this approach for the challenging problem of transport in strongly interacting models, especially those with disorder.

I. INTRODUCTION AND OVERVIEW

Measurements of electrical and thermal currents provide a rich set of data about a quantum many-body system[1–5]. These measurements inform us about not just equilibrium thermodynamic physics but also about sources of dissipation, scattering timescales, and the number and nature of conservation laws. Treating all of these pieces appropriately makes calculation of electrical and thermal currents in many-body systems challenging. For weakly interacting systems with a quasiparticle description a kinetic equation may suffice, but the lack of quasi-particles in many strongly interacting systems means that a kinetic equation will generally fail. Hydrodynamics provides a good description of the long wavelength physics, but the calculation of the transport coefficients is still difficult in general[3]. Numerical approaches are difficult for a variety of reasons, for example, the real time nature of the physics is in tension with imaginary time approaches. Direct time evolution of the many-body state is also computationally infeasible in all but a select set of physical problems[6].

The main idea of this work is that direct time evolution of the many-body state is actually possible using entanglement-based methods with the proper physical setup. The key physical idea is that non-equilibrium steady states (NESS)[7–9] are lightly entangled states in many contexts, at least if they are near equilibrium[10]. In more detail, one would not expect substantially more entanglement than in the ground state and in many cases, e.g. at finite temperature or in contact with leads, there may be substantially less entanglement than in the ground state[11]. Given recent progress demonstrating that ground states are relatively lightly entangled, the claim that current carrying NESS are also lightly entangled seems plausible. The small degree of entanglement then strongly suggests that such NESS should have efficient tensor network representations.

We establish the claim that near-equilibrium NESS are lightly entangled for a wide variety of system using tools from quantum information theory, specifically the rapidly developing theory of approximate quantum Markov chains. Once we know the NESS is lightly entangled and has an efficient tensor network representation, the question becomes how to find the NESS? There are a number of approaches to this problem including variational and dynamical; here we focus on the latter possibility, e.g. determining the NESS by dynamically evolving the system to its steady state. To understand the basic physics of this approach we focus on a simple free-fermion model; this enables us to understand how to model the bath, to probe the temperature range accessible to our methods, and investigate the time needed to reach the steady state (which is expected to be slow) all in a well-studied model. In future papers we add in the machinery of tensor networks to the open system dynamics to treat strong interactions and investigate variational methods to find the NESS.

To model the dynamics of the system coupled to an environment we use markovian dissipative dynamics. The density matrix ρ of the system of interest is assumed to

evolve according a Linblad equation

$$\partial_t \rho = [-iH, \rho] + \sum_j L_j \rho L_j^\dagger - \frac{1}{2} \sum_j \{L_j^\dagger L_j, \rho\}. \quad (1.1)$$

Here H is an effective Hamiltonian describing the evolution of the system and the L_j are so-called jump operators which describe the dissipative effects of the environment.

Our ultimate goal is to solve hard problems in the area of quantum transport. The first message of this paper is that for many physically relevant situations, non-equilibrium steady states are lightly entangled and can be described efficiently using a classical computer. The second message is that the non-equilibrium steady state can be found using open system dynamics. The time to reach the steady state may be slow, but in principle by combining the two messages we can simulate the transport dynamics of strongly interacting and even disordered systems. This is because the methods we employ do not require the existence of quasi-particles, weak coupling, or translation invariance. Furthermore, although the approach is expected to be easiest at high temperature (lowest entanglement), there is no obvious obstruction to studying low temperatures since the tensor network methods we discuss smoothly go over to ground state methods.

To put our work in context, note that despite many approaches for treating non-equilibrium steady states[1,2,12–18], development of new methods remains an active field of research. Many of the ideas we build on have a rich history in quantum many-body physics. The entanglement based approach to ground states, thermal equilibrium states, and even non-equilibrium steady states is well established in one spatial dimension[11,19–22]. There is numerical evidence[10,23–28] and evidence from integrable systems[7,29–37] that NESS can be described using various kinds of matrix product states . Both unitary real time evolution and open system evolution can also be carried out in the context of MPS[6,38–40]. The open system approach to transport is also well trod. However, such approaches often make a mean-field or quasi-particle approximation or take an exact diagonalization approach which is not scalable[24]. There are also a few discussions of open system dynamics and NESS in higher dimensions[41,42].

Our specific interest is transport in strongly correlated systems. Here much attention has recently been paid to effects such as inelastic scattering due to electron phonon coupling, Coulomb blockades, and non-equilibrium Kondo effects. Theoretically there are a variety of different techniques that can be used to treat NESS. One of the most widely used methods is non-equilibrium Green's function approach, which can be used quite generally, but it is essentially a perturbative scheme, and is not expected to be accurate for interacting systems[43]. There are many sorts of quantum Monte Carlo techniques that can treat interacting systems, but they are generally only suitable for imaginary time propagation, and are not always accurate for strongly correlated systems. Even in 1D, where quantum Monte Carlo simulations are exact for ground state simulations, DMRG can generally be used in a much more efficient manner. There has been some progress for developing real time propagation with a quantum Monte Carlo framework that has the potential to work for general Hamiltonians[12]. However sampling and sign problem issues[44] have to be considered for each Hamiltonian individually. Exact diagonalization of course is only feasible for the smallest systems.

Several quantum evolution tools for solving non-equilibirum systems have been developed to directly solve Linblad master equations[45–48]. A comparison of integral, exact diagonalization, and Monte Carlo techniques, demonstrated that for small systems direct diagonalization and integral techniques are the most efficient methods to use. In this benchmark study of Heisenberg spin chains[48], once a critical system size is reached, roughly about 10 sites, wave function Monte Carlo becomes a more efficient method, and has much better scaling properties with system size. However, even Monte Carlo, as discussed above, is not always suitable for strongly correlated systems, and can be computationally expensive for large systems.

As an alternative, the use of MPOs to treat NESS looks extremely promising, and is the technique we consider in this work. There has significant efforts to develop MPOs explictly for time evolving the Linblad equation. For ground state systems MPOs are effective for solving systems with low entanglement in one dimension, which includes strongly correlated systems. It usage for 2D systems also shows its promise of being one of the most efficient methods for certain classes of systems. The use of MPO for solving NESS applications had been originally proposed in the context of bulk disspation[38]. Since then it has been applied to a number of different models. The use of MPOs also allows for in depth theoretical studies of the properties that a solution of a NESS can realize. For instance, when assuming an MPO ansatz for the solution of a NESS, various properties can be proved for both spin systems[34,49], and for Hubbard model systems[37]. For spin systems, numerical results have been used to study integrable and non-integrable models for system sizes on the order of hundreds of sites such as in the Heisenberg XXZ Hamiltonian[31] and the Heisenberg XY[33,50]. A push towards numerical studies of Hubbard models have also been of recent interest. Solving the ground state Hubbard model is still an open field in 2 and 3 dimensions, where exact solutions are not possible, and proper solutions are still debated. Regardless, there have been some studies of NESS for the Hubbard model, such as looking at the transport in the Hubbard model at infinite temperature. These simulations have also been performed with system sizes on the order of hundreds of sites[32]. This is an active field, as the current state of the art has important limitations. Improving accuracy, using larger system sizes, and reaching lower temperatures are open problems that need

to be addressed with improved numerical techniques.

Our paper is organized as follows. In Section 1 we discuss the previous techniques of treating non-equilibrium systems, and specifically focus on previous entanglement approaches. In Section 2 we show that NESS are lightly entangled and prove the existence of efficient tensor network representations under a variety of reasonable assumptions. We also argue that holographic models of transport are naturally situated within our framework[51–54]. If the open system time evolution is adiabatic so that the system stays near its steady state at all times, then the system stays within the manifold of lightly entangled tensor network states discussed above. More here ...

II. ENTANGLEMENT AND CURRENTS IN A FREE FERMION MODEL

In this section we introduce a toy model consisting of fermions moving in a one dimensional wire.

A. Currents and entanglement from low energy theory

Suppose we have a piece of wire of length L containing a spin-less fermion field $c(x)$ and suppose each end of the wire is coupled to a large fermion bath. The left L and right R baths have temperatures $T_{L(R)}$ and chemical potentials $\mu_{L(R)}$. The two point function of fermion operators within the wire is

$$\begin{aligned} G(x,y) &= \langle c^\dagger(x)c(y)\rangle \\ &= \int \frac{dk}{2\pi} e^{-ik(x-y)}\theta(k) f(E_k-\mu_L,T_L) \\ &+ \int \frac{dk}{2\pi} e^{-ik(x-y)}\theta(-k) f(E_k-\mu_R,T_R) \end{aligned} \quad (2.1)$$

where

$$f(E,T) = \frac{1}{e^{E/T}+1} \quad (2.2)$$

is the Fermi function. If $\mu_L = \mu_R$ and $T_L = T_R$ then this describes a wire in equilibrium at temperature T and chemical potential μ. More generally, the above two point function represents a fermion system with the right movers equilibrated with a left bath (from which they originated) and the left movers equilibrated with a right bath (from which they originated).

To illustrate the physics suppose that $\mu_L = \mu_R$ but $T_L > T_R$. Linearize the energy about about μ and call the Fermi velocity v_F (which may in general depend on energy and differ between left and right). The particle current is $I = 0$ while the energy current is $I_E \propto T_L^2 - T_R^2$ (see Appendix A).

How much entanglement is present in this current carrying state? Conformal field theory supplies the answer in the long-wavelength low energy limit [cite]. In terms of the left and right central charges $c_{L,R}$ and the left and right temperatures $T_{L,R}$ the entropy of an interval of length L is

$$\begin{aligned} S(L) = & \frac{c_L}{6}\log\left(\frac{\sinh\left(\frac{\pi T_L L}{v_F(\mu_L)}\right)}{\pi T_L a/v_F(\mu_L)}\right) \\ & + \frac{c_R}{6}\log\left(\frac{\sinh\left(\frac{\pi T_R L}{v_F(\mu_R)}\right)}{\pi T_R a/v_F(\mu_R)}\right) \end{aligned} \quad (2.3)$$

where a is a UV cutoff. This formula allows for the possibility that the Fermi velocity depends on the chemical potential (as it will in general). It demonstrates that even if $\mu_L \neq \mu_R$ and $T_L \neq T_R$ the entanglement structure is qualitatively the same as the thermal state (or ground state) at the appropriate temperature.

Given these entropies the mutual information of the left half the wire, $x \in [0, L/2]$, with the right half of the wire, $x \in [L/2, L]$, can be computed. It is

$$\begin{aligned} & \mathcal{I}([0,L/2],[L/2,L]) \\ & = S([0,L/2]) + S([L/2,L]) - S([0,L]) \\ & \approx \frac{c_L}{6}\log\left(\frac{v_F(\mu_L)}{2\pi T_L a}\right) + \frac{c_R}{6}\log\left(\frac{v_F(\mu_R)}{2\pi T_R a}\right) \end{aligned} \quad (2.4)$$

up to exponentially small corrections. It is identical to ground state mutual information formula with the region size replaced by the thermal correlation length $\xi(T) = \frac{v}{2\pi T}$.

What about in higher dimensions? The analog of the biased wire is a boosted Fermi surface, i.e. a current carrying metallic state. Solution of the Boltzmann equation shows that the state of a metal in a uniform electric field is the same as the equilibrium state but with all momenta shifted by $\vec{Q} = e\vec{E}\tau$ with e the particle charge, $\vec{E}$ the electric field, and τ the relaxation time. Typically this scattering time comes from phonons or impurities, both of which will modify the state of the system in a non-trivial way, but for the purpose of the example we abstract away this extra complication and study just the boosted state.

Two states related by such a momentum shift are connected by a simple unitary transformation given by

$$U_Q = \exp\left(i\sum_j Q_j \int d^d x\, x^j c^\dagger(x)c(x)\right). \quad (2.5)$$

Observe, however, that U_Q is actually a product of local unitaries,

$$U_Q = \prod_x \exp\left(i\sum_j Q_j x^j c^\dagger(x)c(x)\right), \quad (2.6)$$

so application of U_Q to a state does not change the entanglement properties of the state. This establishes that

all entropies of the boosted state are the same as they were in the equilibrium state.

In particular, the mutual information between a region A and its complement $\bar{A}$ is given by the mutual information in the equilibrium state. This equilibrium mutual information may be calculated using the machinery in [cite fs] and is given in d spatial dimensions by

$$\mathcal{I}(A,\bar{A}) \sim k_F^{d-1}|\partial A| \log\left(\frac{E_F}{T}\right). \tag{2.7}$$

Hence in any dimension current carrying metallic states are lightly entangled in the sense of having area law mutual information.

B. The dissipative free fermion problem

So far dynamics have played little role in our analysis. In this section we briefly set up the dynamical free fermion model we consider below. Although the free fermion model can be solved using tensor network methods, we take the simpler route of correlation matrix techniques. This has the advantage of letting us explore the physics of the open system setup without the technical complications of tensor network methods.

The fermion problem is specified by giving a list of fermion annihilation operators $\{c_\alpha\}$ and a Hamiltonian H and a set of jump operator L_j built from the fermion operators. In order for the many-body fermion problem to reduce to a single particle problem the Hamiltonian must be quadratic in c and $c^\dagger$ and the jump operators must be linear in c and $c^\dagger$. Hence we may write the Hamiltonian as

$$H = c^\dagger h c \tag{2.8}$$

and the jump operators as either

$$L_j = u_j^\dagger c \tag{2.9}$$

or

$$L_j = c^\dagger v_j. \tag{2.10}$$

The physics setup of interest to us corresponds to Hamiltonian dynamics in the bulk a sample plus dissipative jump operators acting only at the boundary of the sample.

Assuming the fermion state ρ is Gaussian, that is of the form $\rho \sim e^{-c^\dagger k c}$, all physical quantities can be computed from the correlation matrix $G_{\alpha,\beta} = \mathrm{tr}(c_\alpha^\dagger c_\beta \rho)$. Plugging the above forms of H and L_j into the Linblad equation and assuming the fermion state is Gaussian it is possible to derive (see Appendix) an equivalent equation of motion for the correlation matrix. The result is

$$\partial_t G = i[h^T, G] - \frac{1}{2}\sum_j \left\{u_j^* u_j^T, G\right\} + \frac{1}{2}\sum_j \left\{v_j^* v_j^T, 1-G\right\}. \tag{2.11}$$

Knowing the time dependence of the correlation matrix is sufficient to compute densities, currents, and entropies at all times. It also bears repeating that we could have approached this problem using tensor network methods (indeed, we check below that the conditions discussed above for the existence of a tensor network are fulfilled), but to focus on the physics of the open system we use the simpler correlation matrix approach. To investigate the physics the free fermion open system setup we will consider two models, one which we solve numerically and one which is a simple analytically solvable toy model.

C. Multi-site model

Consider for simplicity a one dimensional wire system composed of three parts. The left contact, the right contact, and the middle of the wire. The bare Hamiltonian for each piece of the wire is taken to be the same free fermion hopping model given by

$$H_0 = \sum_x -w c_x^\dagger c_{x+1} - w c_{x+1}^\dagger c_x. \tag{2.12}$$

The three segments of wire are then coupled by a weak link of strength w'. Finally, we add jump operators in the L and R regions which drive those regions to the thermal state of their respective bare Hamiltonians (without the coupling).

Note that chemical potentials are not included in the Hamiltonian H_0. These potentials can be directly included in the jump operators which couple to the left and right contacts; the physical idea being that by raising or lowering the average $((\mu_L + \mu_R)/2)$ chemical potential and letting the system relax to equilibrium we can set the overall density as desired.

We may also generalize this model slightly by allowing more general system-bath couplings (will remaining within the free fermion context). For example, we may consider further neighbor hoppings between system (wire) and bath (contacts where jump operators act). The effect of such couplings will be to increase the speed of equilibration and to help select the thermal state as the unique fixed point (see below).

In section II E we make a detailed numerical study of this model. Interesting features include recovery of many results from the scattering theory of 1d transport, recovery of diffusive transport in the presence of disorder, and observation of quantum coherence at low temperatures. We mainly use a real time algorithm to find the steady state despite the existence of other methods for free fermions BGS: mention Prosen's work here . This has the advantage that it is immediately generalizable to interacting systems using tensor networks. Thus insights into the timescale of equilibration and algorithmic developments in the free fermion case may shed light on the more physically interesting case of interacting fermions. We check our calculations using a different root finding algorithm as well.

D. Solvable two-site model

To gain further intuition it is useful to solve the general two site model. The jump operators are given by the in rates, $v_L = \sqrt{\gamma}$ and $v_R = \sqrt{\gamma}$, and the out rates, $u_L = \sqrt{\gamma e^{\beta_L(\epsilon_L - \mu_L)}}$ and $u_L = \sqrt{\gamma e^{\beta_R(\epsilon_R - \mu_R)}}$. According to **??** (and in the absence of an LR coupling) these rates lead to equilibrium distributions of the form

$$n_{L,R} = \frac{\gamma_{in}}{\gamma_{out} + \gamma_{in}} = \frac{1}{e^{\beta_{L,R}(\epsilon_{L,R} - \mu_{L,R})} + 1}. \tag{2.13}$$

The above jump operators are already a special case since the base rate γ is taken the same everywhere. We will furthermore assume (without loss of generality) that $\epsilon_{L,R} = 0$ (this may be compensated by $\mu_{L,R}$. Finally, for simplicity take $\beta_{L,R} = \beta$.

The Hamiltonian is taken to be $H = -wc_L^\dagger c_R - wc_R^\dagger c_L$ which translates to a single particle Hamiltonian of the form

$$h = \begin{pmatrix} 0 & -w \\ -w & 0 \end{pmatrix}. \tag{2.14}$$

The single particle quantities controlling the dissipative physics are

$$\sum_j u_j^\star u_j^T = \gamma \begin{pmatrix} e^{-\beta\mu_L} & 0 \\ 0 & e^{-\beta\mu_R} \end{pmatrix} \tag{2.15}$$

and

$$\sum_j v_j^\star v_j^T = \gamma \begin{pmatrix} 1 & 0 \\ 0 & 1 \end{pmatrix}. \tag{2.16}$$

It will be convenient to define $r_0 \pm \delta r = e^{-\beta\mu_{L,R}}$.

The fixed point equation following from 2.13 is thus

$$0 = -iw[X, G] - \frac{1}{2}\{\gamma r_0 + \gamma\delta r Z, G\} - \frac{1}{2}\{\gamma, G - 1\}. \tag{2.17}$$

To simplify notation we have switched to using the Pauli operators $\sigma^i \sim X, Y, Z$ and the identity 1. The equation is most easily solved by resolving G in the Pauli basis,

$$G = a_0 + a_y Y + a_z Z, \tag{2.18}$$

with no X term needed. Using $\{1, \sigma^i\} = 2\sigma^i$, $\{\sigma^i, \sigma^j\} = 2\delta^{ij}$, and $[\sigma^i, \sigma^j] = 2i\epsilon^{ijk}\sigma^k$ the fixed point equation becomes

$$\begin{aligned} 0 = &-iw(2ia_y Z - 2ia_z Y) - \gamma(1 + r_0)(a_0 + a_y Y + a_z Z) \\ &-\gamma\delta r(a_0 Z + a_z) + \gamma. \end{aligned} \tag{2.19}$$

Setting the coefficients of 1, Y, and Z equal to zero gives

$$1 : \ 0 = -\gamma(1 + r_0)a_0 - \gamma\delta r a_z + \gamma, \tag{2.20}$$

$$Y : \ 0 = -2wa_z - \gamma(1 + r_0)a_y, \tag{2.21}$$

and

$$Z : \ 0 = 2wa_y - \gamma(1 + r_0)a_z - \gamma\delta r a_0. \tag{2.22}$$

Solving this set yields

$$a_y = -\frac{2w}{\gamma(1 + r_0)}a_z, \tag{2.23}$$

$$a_0 = \frac{1}{\gamma\delta r}\left(-\frac{4w^2}{\gamma(1 + r_0)} - \gamma(1 + r_0)\right)a_z, \tag{2.24}$$

and

$$a_0 = \frac{1 - \delta r a_z}{1 + r_0}. \tag{2.25}$$

A little further manipulation gives

$$a_z = \delta r\left(-\frac{4w^2}{\gamma^2} - (1 + r_0)^2 + \delta r^2\right)^{-1}. \tag{2.26}$$

Note that a_z is negative if δr is positive as is expected since then $\mu_L < \mu_R$ and hence $n_L < n_R$. It also follows that

$$a_y = \frac{2w}{\gamma(1 + r_0)}\frac{\delta r}{\frac{4w^2}{\gamma^2} + (1 + r_0)^2 - \delta r^2}. \tag{2.27}$$

The current (units of 1/time or energy) is then simply

$$I = -wa_y = -\frac{2w^2}{\gamma(1 + r_0)}\frac{\delta r}{\frac{4w^2}{\gamma^2} + (1 + r_0)^2 - \delta r^2}, \tag{2.28}$$

so if $\delta r > 0$ so that $n_L < n_R$ then $I < 0$ and current flows from R to L.

This equation for the current displays a lot of rich physics. Let us analyze some of it in the linear response limit of $\delta r \ll 1$. Then we can see the physics of the various rates very clearly. If $w \gg \gamma$ then the current goes like $I \sim \gamma\delta r$ indicating that the bottleneck to charge flow is charge input from the dissipation. On the other hand, if $w \ll \gamma$ then the current goes like $I \sim w^2\delta r/\gamma$ and the rate of charge transfer between L and R is the rate limiting step. The current drops to zero as $\gamma \to \infty$ because the left and right sites are then strongly forced to their equilibrium states.

E. Fermion transport data

Discuss scattering theory results, role of bath size, and prefactor.

Discuss coherence and scattering theory results.

Discuss crossover from ballistic to diffusive to localized.

Define geometry better, additional entropy plots, mutual information in disordered system.

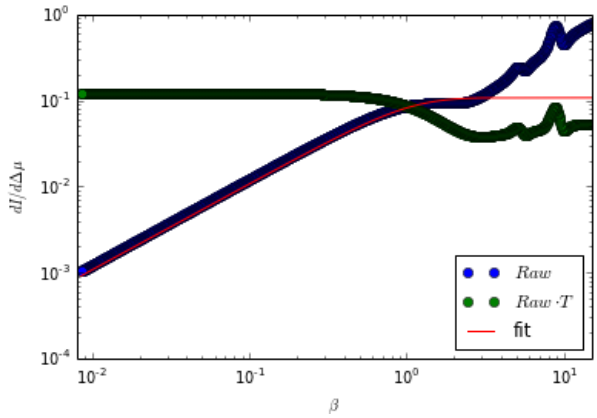

FIG. 1. Linear response electrical conductivity as a function of temperature.

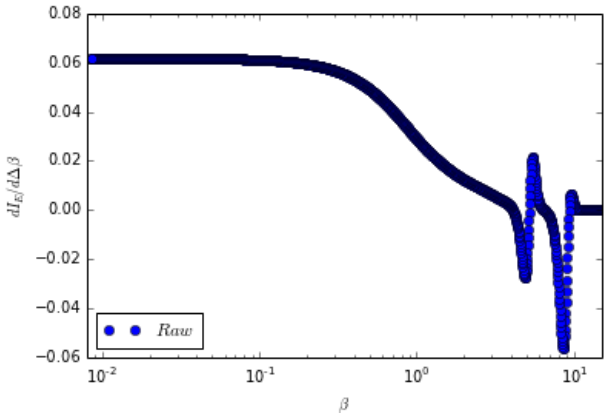

FIG. 2. Linear response thermal conductivity as a function of temperature.

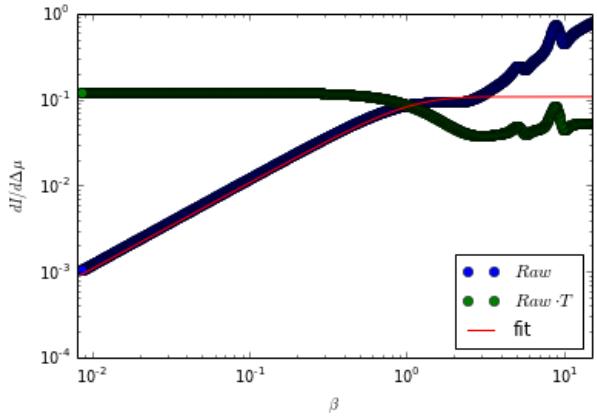

FIG. 3. Current as a function of flux at low temperature.

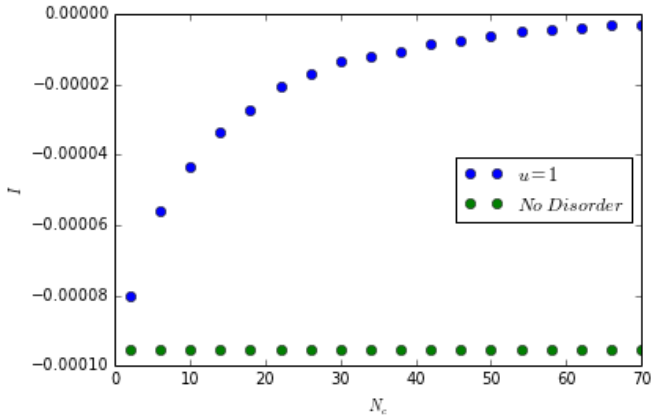

FIG. 4. Current for two different disorder strengths as a function of system size.

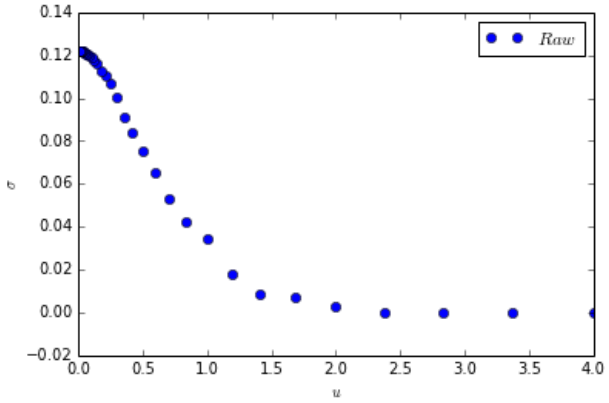

FIG. 5. Electrical conductivity versus disorder strength.

III. ENTANGLEMENT AND CURRENTS IN GENERAL THERMALIZING MANY-BODY SYSTEMS

A. Main assumption: existence of local thermal equilibrium

Above we established that NESS were lightly entangled states in the limit of extreme weak coupling and extreme strong coupling. The weak coupling example is obviously integrable and much is known about the behavior of NESS in integrable systems [cite]. But is the holographic example indicative of the general features of non-integrable models? Intuitively the answer is yes because ultimately what we require is only that the system reach local thermal equilibrium. Provided the system is not integrable, there should exist a finite time τ_{local} to reach local thermodynamic equilibrium. Correspondingly, away from classical critical points (for this case see [Halperin et al.]) correlations will decay, so the notion of local thermal equilibrium is sensible within a derivative

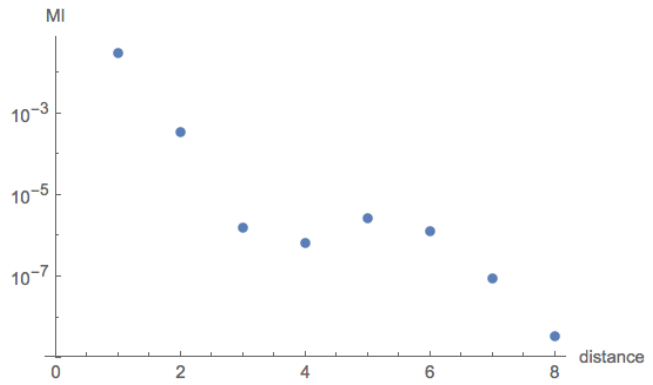

FIG. 6. Mutual information as a function of distance.

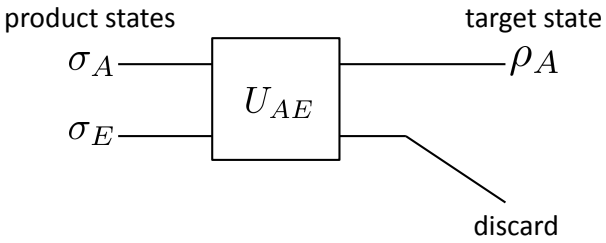

$$\rho_A = \mathrm{tr}_E(U_{AE}\sigma_A\sigma_E U_{AE}^\dagger)$$

FIG. 7. Quantum channel which prepares the state ρ_A from a product state on AE after acting with a local unitary U_{AE} and discarding E.

expansion. Provided the effective local temperature, effective local chemical potential, etc. vary slowly on the scale of the correlation length, a local equilibrium state should provide a good approximation to the state of the system.

Hence we expect that to a good approximation the NESS of an interacting system should be describable by a local equilibrium state of the form

$$\rho_{\text{NESS}} = \frac{\exp\left(-\int d^d x \beta(x)\mathcal{E}(x) + ...\right)}{Z_{\text{NESS}}} \tag{3.1}$$

where $\mathcal{E}(x)$ is the energy density, $\beta(x)$ is a position dependent inverse temperature, ... denotes further local operators like currents and densities, and Z_{NESS} denotes a non-equilibrium partition function. But what can we say about the entanglement structure of such a local equilibrium state?

Verstraete et al. have shown that any density matrix of the form $\rho \sim \exp(-\sum_x O_x)$ has bounded mutual information between a spatial region A and its complement $\bar{A}$. They show that $\mathcal{I}(A,\bar{A}) \propto |\partial A|$ with the coefficient depending on the size of the operators O_x. For a thermal equilibrium state of a local Hamiltonian the bound reads $\mathcal{I} \leq \frac{J}{T}\frac{|\partial A|}{a^{d-1}}$ where J is the energy scale of the microscopic Hamiltonian, T is the temperature, and a is the UV cutoff (lattice spacing).

In fact, this bound, which diverges as $T \to 0$, is often quite loose. For $1+1$d CFTs the mutual information scales like $\mathcal{I} \sim \log\left(\frac{1/T}{a}\right)$ which does diverge as $T \to 0$ but only very weakly. For higher dimensional CFTs the mutual information remains finite, roughly $\mathcal{I} \sim |\partial A| a^{1-d}$, even at $T = 0$. Fermi liquid mutual information also only diverges as $\log\left(\frac{E_F}{T}\right)$ as $T \to 0$. These examples can all be understood as a consequence a generalized renormalization group structure which leads to considerably less mutual information (in terms of the scaling with T) than would be naively expected based on the microscopic physics.

Following this discussion our main assumption is this: near equilibrium current carrying states in interacting models are in local thermal equilibrium. As a consequence, entropies and correlations behave as they do in thermal equilibrium up to corrections which are controlled in a derivative expansion. In particular, the entropy of a region A is assumed to have the form

$$S(A) = c_1|A| + \int_{\partial A}\left(c_2 + \sum_{i>2} c_i f_i(K,R)\right) + \mathcal{O}(\ell^d e^{-\ell/\xi}) \tag{3.2}$$

where R and K are intrinsic and extrinsic curvatures of ∂A and ξ is a correlation length. This assumption is strong but reasonable and can be demonstrated explicitly in a wide variety of models. In the next section we use this assumption and the theory of approximate quantum Markov chains to demonstrate the existence of tensor network representations for current carrying states. We will also argue that the tensor networks have a renormalization group structure which further simplifies computations.

B. Tensor networks from approximate conditional independence

In this subsection we report a construction demonstrating the existence of efficient tensor networks for NESS under the assumption of local thermal equilibrium. Details of the construction will be presented in [Mixed s sourcery]; here we focus on the basic intuition, the key assumptions, and the meaning of the results for transport calculation.

What we argue is that a state in local thermal equilibrium obeying Eq. 3.2 can be obtained as the output of a local quantum channel. In concrete terms this means that the state ρ_A of interest must be obtainable as follows (see Figure 7):

1. Introduce a product state in an enlarged system AE. AE must share the same geometry as A, i.e. we may add extra degrees of freedom on each site, but the coarse metric properties of A must not be modified.

2. Act with a local unitary transformation on AE. Local is defined with respect to the metric on A which AE inherits.

3. Trace out E to produce a state on A.

The range of the local unitary in Step 2 is of order the correlation length, however, below we discuss a further RG decomposition into truly short-ranged (microscopic scale) transformations. This additional RG structure is physically meaningful, but the basic message that an efficient tensor network exists is independent the decomposition (although the decomposition leads to a more efficient network). Finally, as discussed in more detail in [mixed] correlations in such a state can be computed efficiently and the state can represented as an approximate mixed state tensor network, an MPO in 1d or a PEPO in 2d and beyond.

To understand the construction we must introduce some notation. Given three regions A, B, and C, we say that A is conditionally independent of C given B if the condition mutual information, $\mathcal{I}(A:C|B)$, vanishes:

$$\mathcal{I}(A:C|B) = S(AB) + S(BC) - S(B) - S(ABC) = 0. \tag{3.3}$$

For classical random variables this occurs when the probability satisfies $p(a,b,c) = p(a,b)p(b,c)/p(b)$. The consequence classically is the full probability may be obtained from the marginals, that is $p(a,b,c)$ can be reconstructed from just $p(a,b)$ and $p(b,c)$. The reconstruction is just Bayes' rule:

$$\begin{aligned} p(a,b,c) &= p(c|b,a)p(a,b) \\ &=_{\mathcal{I}=0} p(c|b)p(a,b) = \frac{p(c,b)}{p(b)}p(a,b). \end{aligned} \tag{3.4}$$

There is a quantum analogue of the classical reconstruction theorem, namely that if $\mathcal{I}(A:C|B) = 0$ then there exists a quantum channel $\mathcal{N}_{B\to BC}$ such that $\mathrm{Id}_A \otimes \mathcal{N}_{B\to BC}(\rho_{AB}) = \rho_{ABC}$ [cite petz]. Moreover, recently it has been shown that this reconstruction theorem is approximately true provide $\mathcal{I}$ is approximately zero [cite fawzi-renner]. We observe that with a suitable choice of geometry, NESS in local equilibrium often have $\mathcal{I} \approx 0$, so an approximate reconstruction is possible.

Again, what this means in practical terms is that the thermal state can be obtained from a product state by introducing an environment, acting with a local unitary on the system plus environment, and then tracing out the environment. Equivalently, there is a purification of the thermal state which can be constructed from a product state using a local unitary transformation. The actual construction proceeds by introducing a "fattened" cellular decomposition of space. Here fattened means

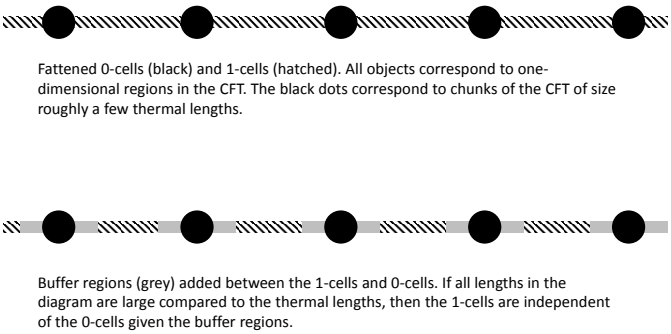

FIG. 8. Setup of the approximate conditional independence construction in 1d.

that all the cells have thermal scale thickness (to avoid non-vanishing short-range correlations disrupting the argument. Then if the state of the n-cells is conditionally independent of the state of the $n-1$-cells given an interface for all n the thermal state is the output of a short-range quantum channel and has an efficient tensor network representation.

As an example, consider a $1+1$d CFT at finite temperature. As reviewed above, the entropy of a region of length ℓ is

$$S(\ell, T) = \frac{c}{3}\log\left(\frac{\sinh(\pi T\ell)}{\pi T a}\right) \tag{3.5}$$

where the velocity has been set to 1 and a is again the UV cutoff. Now suppose $A = [0,\ell]$, $B = [\ell, 2\ell]$, and $C = [2\ell, 3\ell]$. The conditional mutual information is

$$\mathcal{I}(A:C|B) = \frac{c}{3}\log\left(\frac{\sinh^2(2\pi T\ell)}{\sinh(\pi T\ell)\sinh(3\pi T\ell)}\right) \approx 0 \tag{3.6}$$

provided $\ell \gg 1/T$. This implies that the state of ABC can be reconstructed from the state of AB and BC using a local channel of range ℓ.

To reconstruct all of space we decompose the line into a sequence of intervals as shown in Figure 8. Then if the state of the 1 cells is independent of the state of the 0 cells given an interface region, then there exists a quantum channel which approximately attaches the 1 cells to the 0 cells using only local operations. In fact, all the theorem guarantees is that there is a channel acting simulataneously on all the 1 cells (but just the 1 cells) which performs the reconstruction, but because the mutual information between different 1 cells is approximately zero the reconstruction channel may be chosen to be local. And again, this all follows provided the regions involved, including interface regions, are sufficiently large compared to the thermal scale.

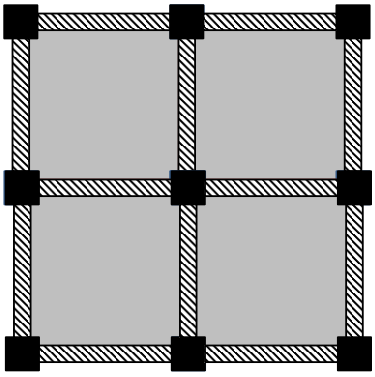

FIG. 9. Setup of the approximate conditional independence construction in 2d. The system is assembled starting from the black 0 cells by adding the hatched 1 cells and finally the grey 2 cells.

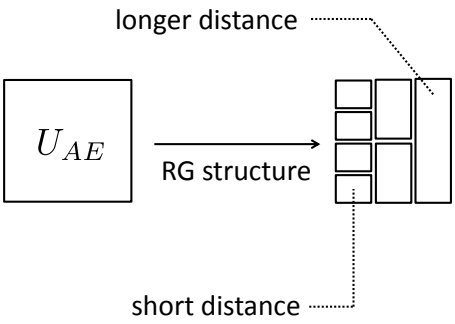

FIG. 10. Setup of the approximate conditional independence construction in 2d. The system is assembled starting from the black 0 cells by adding the hatched 1 cells and finally the grey 2 cells.

The picture is then that the state of the system is built from thermal scale pieces assembled using local operations. Below we discuss a renormalization argument which indicates that the thermal scale pieces may themselves be assembled hierarchically from strictly local (local at the microscopic scale, not just local at the thermal scale) pieces.

Of course, the argument also generalizes immediately to higher dimensions; see Figure 9 for the setup in 2d. As before, provided Eq. 3.2 is obeyed then the relevant conditional mutual informations and mutual informations are approximately zero and approximate local reconstruction channels exist. The reconstruction channels are only guaranteed to be local at the thermal scale, but we argue below that they have an additional hierarchical RG-like structure.

C. Renormalization group structure of tensor networks

In the previous subsection we showed that with the physically reasonable assumption of local thermal equilibrium current carrying steady states have tensor network representations. However, all the previous discussion guaranteed was that the state could be prepared using some general thermal scale operations. Because at low temperature the thermal length scale is quite long compared to microscopic scales, the general thermal scale result is not sufficient to guarantee a computationally efficient (practically speaking) tensor network. However, in both the free fermion and holographic examples there is an additional renormalization group structure which permits to further decompose the thermal scale operations into a sequence of microscopic scale operations which are together much more efficient than a general thermal scale operation. We conjecture that this renormalization group structure generalizes beyond the examples given and give some evidence for the conjecture.

Take first the case of free fermions in 1d. There it is known from numerical studies [cite] that there exist approximate microscopic range unitary transformation which take the ground wavefunction on a size L system into the ground state wavefunction on a size $L/2$ system times some extra product states. This unitary transformation can be interpreted as a kind of renormalization group transformation. Considering the ground state of a size L system, the RG transformation can be repeated roughly $\log_2 L$ times before the system shrinks to microscopic size. Starting from the final factorized state and applying the unitaries in reverse then produces a $\log_2 L$ depth circuit which prepares the ground state.

Since the short-distance correlations in the ground state are not strongly modified by non-zero temperature, the following picture then presents itself for thermal states. The thermal state can also be produced from a product state defined at the thermal scale by applying a sequence of RG circuits which build in the short-distance (shorter than thermal scale) correlations. What this means for our construction above is that the general thermal scale unitary transformation which we showed constructs the thermal state can be further decomposed into short-range pieces as in Fig. **??**. The result approximates the ground state circuit cutoff at the thermal scale (plus some additional mixing between A and E at the thermal scale which produces the entropy of ρ_A).

Now consider the case of the strongly interacting holographic model. As argued in [ent-ren-holo] the holographic geometry may also be understood as being composed of a renormalization group circuit. Then in so

far as the black hole cuts off the holographic geometry deep inside the bulk relative to the ground state geometry while essentially presevering the geometry near the boundary, we may also speculate that a modified version of the ground state circuit with an infrared cutoff at the thermal scale can construct the ground state from a product state. This is of course physically very reasonable.

The general reason why we expect to be able to decompose the general thermal scale unitary into simpler pieces is the unusually low amount of mutual information in the thermal states we consider. Recall that for a conformal field theory the mutual information between a region and its complement is proportional to the area of the region (up to logarithmic corrections), even in the ground state. By contrast, the statement that the thermal state can be produced using thermal scale operations acting on patches of linear size $\xi(T)$ would allow as much as $R^{d-1}\xi$ mutual information for a region of linear size R. Since ξ diverges as the temperature approaches zero, it follows that most of the capacity of a general thermal scale operation is not being used to produce significant correlations. On the other hand, if the RG decomposition we have postulated on physical grounds is valid, then the expected scaling mutual information with temperature and subsystem size is qualitatively reproduced.

D. Coarse-grained versus fine-grained dynamics

Here we briefly comment on the important distinction between closed and open system dynamics and the physical setup in which entanglement ideas are most useful.

Consider a closed quantum many-body system initialized in some out of equilibrium state. To be concrete, we may have in mind a trapped cold atomic gas so that it is reasonable to ignore the coupling to the environment on some physically relevant timescale. On general grounds we expect that such a time evolving closed system will rapidly generate entanglement. Even if the initial state is lightly entangled, say obeying an area law, at late times regions which are not too large will have volume law entanglement. Indeed, if the system exhibits macroscopic thermalization then there is evidence to support the hypothesis that the volume law entanglement entropy reproduces the corresponding thermal entropy.

Assuming the system thermalizes as far as macroscopic observables are concerned, it would be possible to extract a diffusion constant, say, as the atomic gas relaxes to macroscopic equilibrium. However, the presence of a volume law for entanglement entropy means that it would not be possible to simulate the time evolution using entanglement based methods, at least not for very long. A hydrodynamic simulation would be possible, but if our goal is to calculate the diffusion constant by following the dynamics then hydrodynamic simulations will not suffice.

However, suppose the same diffusion constant entering the closed system dynamics also governs diffusion in an open system configuration. As an example of an open system configuration, suppose we permit a density gradient between two well separated environmental contacts. Except for dissipation at the contacts, the dynamics is unitary, and the dynamics of the environment-system composite is presumably still unitary. What this means is that large amounts of entanglement will still be generated, but now we expect, due to the irreversibility of the environment, that the system is predominantly entangled with the environment rather than with itself.

Hence if we are only interested in the state of the system and not the state of the enviroment, it follows from the monogamy of entanglement that the system is not highly entangled amongst its own parts. Nevertheless, we can compute the current between the two contacts using just the state of the system, so the physical information about the diffusion constant is preserved despite the coupling to the environment. We may further imagine beginning the system in equilibrium and slowly biasing the contacts with the environment. If this biasing is done adiabatically then the system will remain close to its non-equilibrium steady state at all times and hence the dynamics can be restricted to the low entanglement states we identified above.

The environment thus acts as a sink for entanglement which preserves the macroscopic transport physics of interest. To recapitulate, assuming the diffusion constant can be measured using both a closed and an open system setup, it makes sense to use entanglement methods to compute the diffusion constant in an open system setup.

IV. DISCUSSION

In this paper we have taken an entanglement-based perspective on the physics of quantum transport. Our main result is to establish a general result on the existence of tensor network representations of non-equilibrium steady states which are in local equilibrium. We also argued that the NESS could be determined by evolving a suitable markovian dynamics until a fixed point is reached. We illustrated this physics with a detailed study of free fermions and compared to known results for the fermion model. Based on these results, we proposed that open system dynamics within a manifold of lightly entangled states is a general framework for the calculation of transport properties of interacting quantum many-body systems.

Indeed, with the guarantee that the NESS has an efficient tensor network representation and assuming the relaxation rate of the Linblad equation is polynomial in system size, then it follows that transport properties of even strongly interacting quantum many-body systems can be computed in time polynomial in system size - a major improvement over exact diagonalization and closed system entanglement methods. Practically speaking it is non-trivial technical challenge to design the right law of dynamical evolution, but here we can appeal to the principle that electrical transport, say, for macroscopic

samples doesn't depend too much on the details of the contact. Working with tensor network states and Linblad dynamics is also a non-trivial technical challenge, one which we address in a future paper.

The systems were we believe the entanglement based approach has the greatest comparative advantage are those with strong correlations which lack a quasi-particle description. Especially difficult is the inclusion of quenched disorder in strongly interacting models, but the entanglement approach is expected to function even better with disorder. Indeed, disorder is known to reduce the average entanglement of a metal from area law violating to area law obeying. Hence disordered strongly interacting non-Fermi liquids provide one ideal target for these methods. We are also interested in thermal transport in strongly coupled conformal field theories in two and three dimensions. Another very tempting target is the infamous linear T resistivity in cuprate superconductors.

In setting up these calculations it is important to correctly incorporate conservation laws. Typically charge is conserved within the sample but can be exchanged with the environment at the boundary. Energy is more subtle; in the fermion examples we consider above energy was also conserved within the sample, but depending on the physical setting it will be more appropriate to allow energy to dissipate in the bulk, e.g. treating phonons as a bulk energy sink. Bulk energy dissipation is interesting since it is expected to further decrease the amount of entanglement present in the NESS and may speed up the approach to equilibrium.

For tensor network calculations there are two primary ingredients. First, we must dynamically evolve within the tensor network variational class. This can be accomplished by applying the Linblad evolution using tensor network operators. The time evolved state is then truncated back into the low entanglement subspace (although we argued above that this truncation shouldn't entail much error). This must all be done while preserving positivity of the density matrix. Second, physical properties of the state must be computed. This is also a non-trivial task for general tensor networks, but the short-ranged nature of entanglement and correlations make this calculation feasible. Preliminary tensor network calculations for several 2d models will be presented elsewhere.

Finally, let us speculate briefly about the larger connections between tensor networks and quantum gravity. Within quantum gravity black holes are interesting for our purposes because they are universal dissipaters (everything falls in) which hide complexity (can't see behind the horizon). We speculate the holographic duality can be understood as a kind of mean field theory of tensor networks. If this is true it becomes interesting to understand how to implement the dissipative and coarse-graining dynamics of a black hole in the tensor network framework. In essence we are looking for a law of dynamical evolution which effectively hides the complex patterns of entanglement that arise in closed system dynamics. Our use of the environment accomplishes this task in the present formulation, but we could hope for a completely intrinsic (to the system in question) dynamical law which would permit us to perform the tensor network analog of letting information fall into a black hole.

Appendix A: Scattering theory approach to 1d ballistic transport

Consider a chain of L sites with Hamiltonian

$$H = \sum_r \left[-w c_r^\dagger c_{r+1} + h.c. - \mu c_r^\dagger c_r \right]. \tag{1.1}$$

The Hamiltonian is easily diagonalized by going to the momentum basis. Writing

$$c_k = \sum_r \frac{e^{ikr}}{\sqrt{L}} c_r \tag{1.2}$$

allows to express the Hamiltonian as

$$H = \sum_k (\epsilon_k - \mu) c_k^\dagger c_k \tag{1.3}$$

where $\epsilon_k = -2w\cos(k)$. We have taken units of length in which the lattice constant is one. The momentum k is confined to the first Brillouin zone $k \in [-\pi, \pi)$. The state labelled by k has a group velocity given by $v_k = \partial_k \epsilon_k = 2w\sin(k)$.

Now the usual picture of transport through such a quantum wire is ballistic. One imagines that right moving particles move through the wire coming from some distant left lead and similarly that left moving particles come from distant right lead. (Don't let the left/right terminology confuse.) When there is no scattering in the wire, then the charge and energy currents are determined simply by the difference in the flows from the left and the right (this assumes that each particle moving from left to right or vice versa is instantly thermalized when it reaches the opposite lead.

This yields the following expression for the currents. The electric current (with the electron charge set to one) from left to right is given by

$$I_{L\to R} = \int_0^\pi \frac{dk}{2\pi} v_k f(\epsilon_k - \mu_L, T_L); \tag{1.4}$$

similarly, the thermal current is

$$I_{E,L\to R} = \int_0^\pi \frac{dk}{2\pi} \epsilon_k v_k f(\epsilon_k - \mu_L, T_L). \tag{1.5}$$

Here f is assumed to be the Fermi function $f(E,T) = (e^{E/T}+1)^{-1}$ although in principle what appears here is simply the distribution function of the left lead (which we assume is thermal).

The corresponding currents from right to left are

$$I_{R\to L} = \int_{-\pi}^0 \frac{dk}{2\pi} v_k f(\epsilon_k - \mu_R, T_R) \tag{1.6}$$

and

$$I_{E,R\to L} = \int_{-\pi}^{0} \frac{dk}{2\pi} \epsilon_k v_k f(\epsilon_k - \mu_R, T_R). \tag{1.7}$$

The total currents are

$$I = I_{L\to R} + I_{R\to L} \tag{1.8}$$

and

$$I_E = I_{E,L\to R} + I_{E,R\to L}. \tag{1.9}$$

Let us first examine the limit of small T. In this case the electrical current reduces to the difference in the chemical potential between left and right. To show this we begin with the formula

$$\lim_{T\to 0} f(E,T) = \theta(-E) \tag{1.10}$$

with $\theta(x)$ the Heaviside step function. Then it follows that

$$\int_0^\pi \frac{dk}{2\pi} \partial_k \epsilon_k \theta(\mu - \epsilon_k) = \int_0^\mu \frac{d\epsilon}{2\pi} = \frac{\mu}{2\pi}. \tag{1.11}$$

Since the velocity has the opposite sign for $k \in (-\pi, 0)$ it follows that the total current is

$$I = \frac{1}{2\pi}(\mu_L - \mu_R). \tag{1.12}$$

A similar calculation reveals that to lowest non-vanishing order the energy current is ($\mu_L = \mu_R = 0$)

$$I_E = \frac{\pi}{12}(T_L^2 - T_R^2). \tag{1.13}$$

What about the opposite limit of very high temperature, $T \gg w$? In this case one may expand the Fermi function as

$$f(E,T) = \frac{1}{2 + E/T} = \frac{1}{2} - \frac{E}{4T} + ... \tag{1.14}$$

The electrical current requires computing the integral

$$\int_0^\pi \frac{dk}{2\pi} v_k \left(\frac{1}{2} - \frac{\epsilon_k - \mu}{4T}\right). \tag{1.15}$$

The first term will cancel when the $R \to L$ current is subtracted and the second term simplifies to

$$\frac{w\mu}{2\pi T}. \tag{1.16}$$

This gives an electrical current of

$$I = \frac{w}{2\pi T}(\mu_L - \mu_R). \tag{1.17}$$

The energy current requires the integral

$$\int_0^\pi \frac{dk}{2\pi} \epsilon_k v_k \left(\frac{1}{2} - \frac{\epsilon_k - \mu}{4T}\right) \tag{1.18}$$

where again the first term will cancel. Now, however, the μ term integrates to zero while the term involving ϵ_k from f survives. The integral evaluates to

$$-\frac{2w^3}{3\pi T}. \tag{1.19}$$

Note that there is a slight subtlety here about whether ϵ_k or $\epsilon_k - \mu$ is the energy being transported; we will discuss this later but one of the advantages of $\mu = 0$ is that this issue is irrelevant. The energy current then is

$$I_E = -\frac{2w^3}{3\pi}\left(\frac{1}{T_L} - \frac{1}{T_R}\right). \tag{1.20}$$

As a check, if $T_L > T_R$ then energy should flow from L to R and so $I_E > 0$ since $1/T_L < 1/T_R$.

We can also ask about electric current with a scattering center in the wire, say a barrier of some height. In this case there will be some probability $\mathcal{T}(E)$ to transmit at energy E as well as a probability $\mathcal{R}(E) = 1 - \mathcal{T}$ to reflect at energy E. The currents (at zero temperature and assuming no energy dependence in $\mathcal{T}$) are then

$$I_{L\to R} = \frac{\mu_L}{2\pi}\mathcal{T} \tag{1.21}$$

and

$$I_{R\to L} = -\frac{\mu_R}{2\pi}\mathcal{T}. \tag{1.22}$$

This expressions arise because the total current from the L lead, say, is $\frac{\mu_L}{2\pi}$, but only a fraction $\mathcal{T}$ makes it through the scatterer with the other fraction being reflected back. The total current is

$$I = I_{L\to R} + I_{R\to L} = \frac{\mathcal{T}}{2\pi}(\mu_L - \mu_R). \tag{1.23}$$

An analogous computation can be carried out for energy currents and for other approximations to $\mathcal{T}$ and choices of T.

Now as a final comment, all these computations apply for the infinite wire with the explicit assumption of left and right thermal equilibrium at infinity. Our model is explicitly a finite wire (which is more physical) which nevertheless should display much of this physics. One possibility for deviations comes from the contact between the lead and the wire which can lead to extra scattering and a contact resistance. Otherwise we expect the above formulas to be well borne out given a sufficiently large wire.

Appendix B: Derivation of Linblad equation in Green's function form

In this subsection we review how in free fermion systems the many-body Linblad equation can be simplified

to a single particle equation for the Green's function (essentially Wick's theorem). Consider a free fermion system with density matrix

$$\rho(t) = \frac{\exp\left(-c^\dagger K(t) c\right)}{Z(t)} \tag{2.1}$$

where $K(t)$ is a time dependent single particle matrix. Such a quadratic fermion state is totally determined by its two point function

$$G_{\alpha\beta}(t) = \mathrm{tr}\left(c^\dagger_\alpha c_\beta \rho(t)\right). \tag{2.2}$$

In fact, one easily finds that

$$G(t) = \frac{1}{e^{K^T(t)} + 1} \tag{2.3}$$

as matrices. Note the transpose, a consequence of the matrix notation. If we diagonalize K and switch to the energy basis, then G is the usual Fermi function.

Now suppose ρ evolves in contact with an environment according to a master equation,

$$\partial_t \rho = -i[H,\rho] + \sum_j L_j \rho L_j^\dagger - \frac{1}{2}\sum_j \left\{L_j^\dagger L_j, \rho\right\}. \tag{2.4}$$

We take H to be quadratic,

$$H = c^\dagger h c, \tag{2.5}$$

and the jump operators L_j are linear in the fermions, e.g.

$$L_j = u_j^\dagger c \tag{2.6}$$

or

$$L_j = c^\dagger v_j \tag{2.7}$$

with u and v column vectors of amplitudes.

Such a master equation preserves the gaussian nature of the state, hence we should be able to understand the dynamics by studying just the equation of motion for G. We compute first the Hamiltonian term. We must evaluate

$$\begin{aligned}
[\partial_t G]_{\mathrm{cons}} &= \mathrm{tr}\left(c_x^\dagger c_y [-iH,\rho]\right) \\
&= \mathrm{tr}\left([c_x^\dagger c_y, -iH]\rho\right) \\
&= -i\sum_{z,w} h_{z,w}\mathrm{tr}\left([c_x^\dagger c_y, c_z^\dagger c_w]\rho\right).
\end{aligned} \tag{2.8}$$

The commutator is

$$[c_x^\dagger c_y, c_z^\dagger c_w] = c_x^\dagger c_w \delta_{y,z} - c_z^\dagger c_y \delta_{x,w}, \tag{2.9}$$

and because we subsequently average over ρ, the final answer may be cast as

$$[\partial_t G]_{\mathrm{cons}} = -i[G, h^T]. \tag{2.10}$$

As a check, if $K = h$, then because $[h^T, h^T] = 0$, G is time independent. Again, note that the appearance of the transpose is just a consequence of the matrix notation and is of no deep significance.

Now we turn to the dissipative terms. The general term in the sum over j (sum over jump operators) is

$$\begin{aligned}
[\partial_t G]_{\mathrm{diss}} &= \mathrm{tr}\left(c_x^\dagger c_y L\rho L^\dagger - c_x^\dagger c_y \frac{1}{2}\left\{L^\dagger L, \rho\right\}\right) \\
&= \mathrm{tr}\left(\left(L^\dagger c_x^\dagger c_y L - \frac{1}{2}\left\{L^\dagger L, c_x^\dagger c_y\right\}\right)\rho\right).
\end{aligned}$$

If $L = u^\dagger c$ then we compute

$$c_a^\dagger c_x^\dagger c_y c_b - \frac{1}{2}\left\{c_a^\dagger c_b, c_x^\dagger c_y\right\} = -\frac{1}{2}\left(c_a^\dagger c_y \delta_{b,x} + c_x^\dagger c_b \delta_{a,y}\right). \tag{2.11}$$

Appending the factors of u and taking the average over ρ we have

$$\begin{aligned}
[\partial_t G]_{\mathrm{diss}} &= \sum_{a,b} -\frac{1}{2} u_b^* u_a \left(G_{a,y}\delta_{b,x} + G_{x,b}\delta_{a,y}\right) \\
&= -\frac{1}{2}\left\{u^* u^T, G\right\}.
\end{aligned} \tag{2.12}$$

If $L = c^\dagger v$ then we find

$$\begin{aligned}
[\partial_t G]_{\mathrm{diss}} &= \frac{v_b v_a^*}{2}\mathrm{tr}\left(\left(c_a c_x^\dagger \delta_{y,b} + c_y c_b^\dagger \delta_{a,x}\right)\rho\right) \\
&= v^* v^T - \frac{1}{2}\left\{v^* v^T, G\right\} \\
&= \frac{1}{2}\left\{v^* v^T, 1 - G\right\}
\end{aligned}$$

If we now add up all terms we find

$$\partial_t G = i[h^T, G] - \frac{1}{2}\sum_j \left\{u_j^* u_j^T, G\right\} + \frac{1}{2}\sum_j \left\{v_j^* v_j^T, 1 - G\right\}. \tag{2.13}$$

This equation completely determines the two point function G which in turn completely determines the state. We can also directly compute the von Neumann entropy of regions using G.

1. Thermal Linblad fixed points for free fermions

In this first subsection we review a construction of jump operators such that the corresponding Linblad equation has as its unique fixed point a free fermion thermal state. We begin with a single mode: given a single fermion mode c with Hamiltonian $H = \epsilon c^\dagger c$, what Linblad operator has the thermal state at temperature T and chemical potential μ as its fixed point?

There will be only two jump operators, $L_1 = \sqrt{\gamma_{in}} c^\dagger$ and $L_2 = \sqrt{\gamma_{out}} c$, so just the ratio of their rates must be determined. The Linblad fixed point equation is

$$0 = -i[H,\rho] + L_1 \rho L_1 + L_2 \rho L_2 - \frac{1}{2}\{L_1^\dagger L_1 + L_2^\dagger L_2, \rho\}. \tag{2.14}$$

If $\rho = \exp(-\beta(H - \mu n))$ is to be a solution, then the Hamiltonian term drops out and only the jump operators contribute.

To find the right rates it helps to use the operator relation $f(n)c = cf(n-1)$ where $n = c^\dagger c$. The equation to satisfy is

$$\gamma_{in} c^\dagger e^{-\beta(\epsilon-\mu)n} c + \gamma_{out} c e^{-\beta(\epsilon-\mu)n} c^\dagger = (\gamma_{in} cc^\dagger + \gamma_{out} c^\dagger c) e^{-\beta(\epsilon-\mu)n}. \quad (2.15)$$

The correct ratio of rates is

$$\gamma_{in} e^{\beta(\epsilon-\mu)} = \gamma_{out}. \quad (2.16)$$

Then for any multimode system (but still free), the same construction immediately generalizes to give a Linblad operator whose fixed point is the thermal state. In more detail, let the single particle Hamiltonian be h with energy levels ϵ_n and single particle wavefunctions ψ_n. The wavefunctions ψ_n are functions of position $\psi_n(x)$ or in our case functions of a discrete position or lattice site label. For each mode ϵ_n we then have a pair of jump operators of the form $\sqrt{\gamma_{in,n}} c_n^\dagger$ and $\sqrt{\gamma_{out,n}} c_n$. Note that $\sum_x \psi_n^*(x) c(x) = c_n$ is just the annihilation operator for the energy mode n. As in the single mode case, the only constraint is that

$$\gamma_{in,n} e^{\beta(\epsilon_n-\mu)} = \gamma_{out,n} \quad (2.17)$$

for all n.

Note: the correct change of basis in an M mode system is easily remembered as follows. The Hamiltonian is $H = c^\dagger h c$. The eigenstates of h are $h\psi_n = \epsilon_n \psi_n$ (remember that h is just an $M \times M$ matrix, while H is a quantum operator on the many-particle Hilbert space). Assemble the eigenvactors of h into a matrix $u_h = [\psi_1, ..., \psi_M]$ and energies into a diagonal matrix $d_h = (\epsilon_1, ..., \epsilon_M)$. Then using $hu_h = u_h d_h$ it follows that

$$H = c^\dagger h c = c^\dagger u_h d_h u_h^\dagger c = (u_h^\dagger c)^\dagger d_h (u_h^\dagger c). \quad (2.18)$$

Hence the correct modes are given by the entries of the vector of operators $u_h^\dagger c$.

2. Review of quantum Markov chains

Here we review the physics of quantum Markov chains, see e.g.[55]. We say a tripartite state ρ_{ABC} forms a quantum Markov chain if the conditional mutual information $I(A:C|B) = S(AB) + S(BC) - S(B) - S(ABC)$ vanishes. Classically this would imply that the probability distribution factorizes, $p(a,b,c) = \frac{p(a,b)p(b,c)}{p(b)}$, so that A is independent of C given B: $p(a,c|b) = \frac{p(a,b,c)}{p(b)} = \frac{p(a,b)}{p(b)} \frac{p(b,c)}{p(b)}$. What is the quantum version of this statement?

Notice that strong subadditivity implies that $I(A:C|B) \geq 0$, so states with $I(A:C|B) = 0$ saturate strong subadditivity. Suppose ρ_{ABC} saturates strong subadditivity and consider a generic perturbation $\rho_{ABC} \to \rho_{ABC} + \delta\rho_{ABC}$. Demanding that the trace of the perturbed state be 1 gives $\mathrm{tr}(\delta\rho_{ABC}) = 0$. Now consider the variation of $I(A:C|B)$ and use $\delta S(\sigma) = -\mathrm{tr}(\delta\sigma \log\sigma) - \mathrm{tr}(\delta\sigma) = -\mathrm{tr}(\delta\sigma \log\sigma)$. We find

$$\delta I(A:C|B) = \mathrm{tr}\left(\delta\rho_{ABC}\left[-\log\rho_{AB} - \log\rho_{BC} + \log\rho_B + \log\rho_{ABC}\right]\right) \quad (2.19)$$

but $I(A:C|B)$ must remain positive for all $\delta\rho$ so the linear term in the variation must vanish,

$$\log\rho_{ABC} = \log\rho_{AB} + \log\rho_{BC} - \log\rho_B, \quad (2.20)$$

which is the quantum analog of $p(a,b,c) = \frac{p(a,b)p(b,c)}{p(b)}$. Note: we have not been careful with the factors, but expressions like $-\log\rho_{BC}$ should be understood as $-I_A \otimes \log\rho_{BC}$ as appropriate.

What about reconstruction? In the classical case we can exactly reconstruct $p(a,b,c)$ from $p(a,b)$ and $p(b,c)$ if the conditional mutual information is zero. The reconstruction is Bayes rule,

$$p(a,b,c) = p(c|a,b)p(a,b) \underbrace{\to}_{I=0} p(c|b)p(a,b) = \frac{p(b,c)p(a,b)}{p(b)}. \quad (2.21)$$

The quantum analog of this statement is Petz's recovery channel.

Consider a quantum channel tr_C which maps ABC to AB by simply tracing out C. This is a valid quantum operation, namely throwing away a system. What is the transpose channel (see previous subsection) of the channel tr_C relative to ρ_{ABC}? The Krauss operators (they are not square matrices) of tr_C are

$$M_c = \langle c|, \quad (2.22)$$

so the Krauss operators of the Petz channel $\mathcal{R}$ (which maps AB to ABC) are

$$M_c^{\mathcal{R}} = \rho_{ABC}^{1/2} |c\rangle \rho_{AB}^{-1/2}. \quad (2.23)$$

These look quite messy, but for quantum Markov chains there is a dramatic simplification. Define $K_R = -\log\rho_R$ and write

$$M_c^{\mathcal{R}} = e^{-K_{AB}/2 - K_{BC}/2 + K_B/2} |c\rangle e^{K_{AB}/2} = e^{-K_{BC}/2 + K_B/2} |c\rangle. \quad (2.24)$$

Note that these depend only on ρ_{BC}.

Let us compute the action of $\mathcal{R}$ on a state σ_{AB}. Using the Krauss operators just derived we have

$$\mathcal{R}(\sigma_{AB}) = \sum_c \rho_{BC}^{1/2} \rho_B^{-1/2} |c\rangle \sigma_{AB} \langle c| \rho_B^{-1/2} \rho_{BC}^{1/2}. \quad (2.25)$$

The sum over c can be performed immediately to yield $I_C = \sum_c |c\rangle\langle c|$, so the channel action is

$$\mathcal{R}(\sigma_{AB}) = \rho_{BC}^{1/2} \rho_B^{-1/2} \sigma_{AB} \rho_B^{-1/2} \rho_{BC}^{1/2} \quad (2.26)$$

which is the Petz map. One can verify that $\mathcal{R}(\rho_{AB}) = \rho_{ABC}$ using the properties of the quantum Markov chain.

We emphasize one point: every pair $\mathcal{E}, \sigma$ defines a recovery channel that reverses the action of $\mathcal{E}$ on σ. What is highly non-trivial here, and essential for the constructions in the main text, is that the Petz map doesn't depend on the state of the whole system but only on the state of the marginals. Combined with the vanishing of the mutual information this demonstrates that the channels above are local.

The recent developments in this field were initiated by Fawzi and Renner[56] who showed that if $I(A:C|B) \approx 0$ then there is an approximate recovery map which acts only on $B \to BC$. Furthermore, it was later shown[57] that this map is independent of ρ_A meaning not only does it not act on the A system, the $B \to BC$ map is also independent of the state on A. This is the machinery we use in our construction.

3. Thermal state as a local Linblad fixed point

The idea here builds on the construction of thermal states using approximate conditional independence. Consider a d dimensional disk D_x centered at position x with radius a few thermal lengths. Let $\mathcal{R}_x$ be the transpose map obtained from the trace map tr_{D_x} using the state $\rho(T)$, $\mathcal{R}_x = \mathcal{R}_{\mathrm{tr}_{D_x},\rho(T)}$. Assuming the thermal state obeys 3.2 then the preceding discussion shows that $\mathcal{R}_x$ can be instantiated as a local map acting in a neighborhood of D_x.

$\mathcal{R}_x$ maps the total system minus the disk to the total system, so it is convenient to define a new map from the total system to the total system. It is simply the composition of $\mathcal{R}_x$ and tr_{D_x},

$$\Phi_x(\sigma) = \mathcal{R}_x(\mathrm{tr}_{D_x}(\sigma)). \tag{2.27}$$

Φ_x has two crucial properites: it obeys $\Phi_x(\rho(T)) = \rho(T)$ and it is local.

We wish to turn this into a dynamical map. The Linblad equation is

$$\partial_t \sigma = \mathcal{L}(\sigma) \tag{2.28}$$

where $\mathcal{L}$ is the Linblad superoperator. Consider a Linblad superoperator defined by

$$\mathcal{L} = \sum_x (\Phi_x - \mathrm{id}). \tag{2.29}$$

Then we compute

$$\partial_t \rho(T) = \mathcal{L}(\rho(T)) = \sum_x (\Phi_x(\rho(T)) - \rho(T)) = 0, \tag{2.30}$$

so $\rho(T)$ is a fixed point of the flow generated by $\mathcal{L}$. With more work it should be possible to show that $\rho(T)$ is the unique fixed and perhaps even bound the mixing time, see [Kastoryano-Brandao].

Besides the intrinsic theoretical interest, this result may have practical applications in the transport project.

[1] S. Datta, *Electronic transport in mesoscopic systems* (Cambridge university press, 1997).

[2] Blandin, A., Nourtier, A., and Hone, D.W., J. Phys. France **37**, 369 (1976), keldysh formalism.

[3] H. Spohn, Rev. Mod. Phys. **52**, 569 (1980), early review, with hydrodynamic references.

[4] A. J. Leggett, S. Chakravarty, A. T. Dorsey, M. P. A. Fisher, A. Garg, and W. Zwerger, Rev. Mod. Phys. **59**, 1 (1987), review paper of dissapative dynamics in two state system.

[5] J. E. Han, Phys. Rev. B **87**, 085119 (2013), from brian.

[6] G. Vidal, Phys. Rev. Lett. **93**, 040502 (2004), real time evolution mps.

[7] T. Prosen, ArXiv e-prints (2015), new review paper, arXiv:1504.00783 [cond-mat.stat-mech].

[8] R. A. Blythe and M. R. Evans, Journal of Physics A: Mathematical and Theoretical **40**, R333 (2007), nESS review.

[9] R. Alicki, in *Dynamics of Dissipation*, Lecture Notes in Physics, Berlin Springer Verlag, Vol. 597, edited by P. Garbaczewski and R. Olkiewicz (2002) pp. 239–264, old review paper with examples, quant-ph/0205188.

[10] J. Cui, J. I. Cirac, and M. C. Bañuls, Phys. Rev. Lett. **114**, 220601 (2015), new techniques, variational principle.

[11] F. Verstraete, J. J. García-Ripoll, and J. I. Cirac, Phys. Rev. Lett. **93**, 207204 (2004), mpo finite temp,discussion of positivity of density matrix.

[12] L. Mühlbacher and E. Rabani, Phys. Rev. Lett. **100**, 176403 (2008), real time path integrals.

[13] M. Pletyukhov, D. Schuricht, and H. Schoeller, Phys. Rev. Lett. **104**, 106801 (2010), non-equilibrium renormalization group.

[14] R. Egger, L. Mühlbacher, and C. H. Mak, Phys. Rev. E **61**, 5961 (2000), real time path integral, spin boson.

[15] K. Mølmer, Y. Castin, and J. Dalibard, J. Opt. Soc. Am. B **10**, 524 (1993), wave function monte carlo reference.

[16] J. Dalibard, Y. Castin, and K. Mølmer, Phys. Rev. Lett. **68**, 580 (1992), wave function monte carlo reference.

[17] C. W. Gardiner, A. S. Parkins, and P. Zoller, Phys. Rev. A **46**, 4363 (1992), wave function monte carlo reference.

[18] T. Prosen, New Journal of Physics **10**, 043026 (2008), method to solve quadratic calculations.

[19] S. R. White, Phys. Rev. Lett. **69**, 2863 (1992), dmrg original paper.

[20] U. Schollwöck, Rev. Mod. Phys. **77**, 259 (2005).

[21] U. Schollwck, Annals of Physics **326**, 96 (2011), january 2011 Special Issue.

[22] M. J. Hartmann, J. Prior, S. R. Clark, and M. B. Plenio, Phys. Rev. Lett. **102**, 057202 (2009), heisenberg dmrg,repreated interactions protocol.

[23] E. Mascarenhas, H. Flayac, and V. Savona, ArXiv e-prints (2015), new technique, implementation of the varitional principle to determine a Ness, prsented in the other two 2015 papers,compares trotter to vartionalal ness, arXiv:1504.06127 [quant-ph].

[24] J. Jin, D. Rossini, R. Fazio, M. Leib, and M. J. Hartmann, Phys. Rev. Lett. **110**, 163605 (2013), mean field and mpo analysis.

[25] H. Weimer, Phys. Rev. Lett. **114**, 040402 (2015), variational ness, dissaptive ising model.

[26] Z. Cai and T. Barthel, Phys. Rev. Lett. **111**, 150403 (2013), interesting results for ising model via dmrg,xxz results versus transverse.

[27] M. Kliesch, D. Gross, and J. Eisert, Phys. Rev. Lett. **113**, 160503 (2014), np hardness for determing whether mpo is physical state.

[28] T. Prosen, Journal of Statistical Mechanics: Theory and Experiment **2010**, P07020 (2010), more exact solutions.

[29] D. Karevski, V. Popkov, and G. M. Schütz, Phys. Rev. Lett. **110**, 047201 (2013), evidence mpo can represent linblad nonequilbirum state, known as the lod method (local operator divergence).

[30] S. R. Clark, J. Prior, M. J. Hartmann, D. Jaksch, and M. B. Plenio, New Journal of Physics **12**, 025005 (2010), repreated interactions protocol.

[31] T. Prosen and M. nidari, Journal of Statistical Mechanics: Theory and Experiment **2009**, P02035 (2009), from brian, dmrg simulations of spin chains.

[32] T. c. v. Prosen and M. Žnidarič, Phys. Rev. B **86**, 125118 (2012), from brian, dmrg simulations of hubbard model.

[33] T. c. v. Prosen, Phys. Rev. Lett. **107**, 137201 (2011), exact solution xxz chain (isolating defect opertor method).

[34] T. c. v. Prosen, Phys. Rev. Lett. **106**, 217206 (2011), non-exact paper of spin chain, same method as other prosen2011 (ido).

[35] T. c. v. Prosen, Phys. Rev. Lett. **112**, 030603 (2014), hubbard model, ido method (isolating defect operator).

[36] T. Prosen, Physica Scripta **86**, 058511 (2012), discussion of uniquness of mpo.

[37] V. Popkov and T. c. v. Prosen, Phys. Rev. Lett. **114**, 127201 (2015), hubbard mode results.

[38] M. Zwolak and G. Vidal, Phys. Rev. Lett. **93**, 207205 (2004), another time dependent reference.

[39] S. R. White and A. E. Feiguin, Phys. Rev. Lett. **93**, 076401 (2004), real time evolution mps.

[40] A. J. Daley, C. Kollath, U. Schollwck, and G. Vidal, Journal of Statistical Mechanics: Theory and Experiment **2004**, P04005 (2004), real time evolution mps.

[41] S. Yan, D. A. Huse, and S. R. White, Science **332**, 1173 (2011), 2d dmrg, http://www.sciencemag.org/content/332/6034/1173.full.pdf.

[42] E. Stoudenmire and S. R. White, Annual Review of Condensed Matter Physics **3**, 111 (2012), 2d dmrg review.

[43] H. Haug and A. P. Jauho, *Quantum Kinetics in Transport and Optics of Semiconductors* (Springer, 1996).

[44] N. M. Tubman, J. L. DuBois, R. Q. Hood, and B. J. Alder, The Journal of Chemical Physics **135**, 184109 (2011).

[45] R. Schack and T. A. Brun, Computer Physics Communications **102**, 210 (1997).

[46] S. M. Tan, Journal of Optics B: Quantum and Semiclassical Optics **1**, 424 (1999).

[47] A. Vukics and H. Ritsch, "C++qed: an object-oriented framework for wave-function simulations of cavity qed systems," (2007).

[48] J. Johansson, P. Nation, and F. Nori, Computer Physics Communications **183**, 1760 (2012), open source wave function monte carlo code in python.

[49] E. Ilievski and T. Prosen, Nuclear Physics B **882**, 485 (2014), lai Sutherland model results.

[50] T. c. v. Prosen and I. Pižorn, Phys. Rev. Lett. **101**, 105701 (2008).

[51] J. Sonner, Journal of High Energy Physics **2013**, 145 (2013), 10.1007/JHEP07(2013)145.

[52] D. Musso, ArXiv e-prints (2014), arXiv:1401.1504 [hep-th].

[53] A. Amoretti, A. Braggio, N. Maggiore, N. Magnoli, and D. Musso, Journal of High Energy Physics **2014**, 160 (2014), 10.1007/JHEP09(2014)160.

[54] R. A. Davison and B. Goutéraux, Journal of High Energy Physics **1**, 39 (2015), arXiv:1411.1062 [hep-th].

[55] P. Hayden, R. Jozsa, D. Petz, and A. Winter, Communications in Mathematical Physics **246**, 359 (2004), quant-ph/0304007.

[56] O. Fawzi and R. Renner, ArXiv e-prints (2014), arXiv:1410.0664 [quant-ph].

[57] D. Sutter, O. Fawzi, and R. Renner, ArXiv e-prints (2015), arXiv:1504.07251 [quant-ph].